國立臺灣師範大學

地球科學系暨研究所

暑期學生專題研究計畫書面報告

Department of Earth Sciences
National Taiwan Normal University
Earth Sciences Summer Student Program Report

臺灣脊樑山脈低傾角夾皺劈理之特性研究

Characteristics Study of Gentle-Dipping Crenulation Cleavages, Eastern Backbone Range, Taiwan

李崇毓

Chung-Yu Li

指導教授：葉恩肇 博士

Advisor: En-Chao Yeh Ph.D.

中華民國 **109** 年 **8** 月

August, 2018

1. Introduction (Purpose)

Gentle dipping crenulation cleavage (S3) can be found in the eastern Backbone Range and its attitude is quite different from the excepted attitude as the ongoing collision between Eurasian and Philippine Sea Plates. Before comprehending the role of S3 in the Taiwan mountain building processes, it is necessary to understand the geometry and kinematics aspects of S3. Therefore, the aim of this study is to analyze the properties of the crenulation cleavages (S3), discusses how they developed, and evaluates the feasibility of dating. The average attitude of crenulation cleavages (S3) is 259.9°/16.4°N from the field data. We further computed the vertical shortening and discuss distribution changes of vertical shortening along the eastern Backbone Range. Also, we compared the vertical shortening of different scales at the same target sample (2020071502) collected from the Mukua River. Nevertheless, we performed Raman Spectroscopy on Carbonaceous Materials (RSCM) analysis on the sample 2020071502 to estimate the maximum metamorphic temperature from the foliation (S2) and the crenulation cleavages (S3), respectively. We showed that the maximum temperature of S2 is 463±30°C and S3 is 472±30°C respectively, and their temperature distributions indicate that S3 has been experienced higher temperature event. This result can be used for exploring the high-temperature event in the future and it suggested that the possibility of obtaining the deformation age is not so good.

2. Geological Setting

2.1 Research area

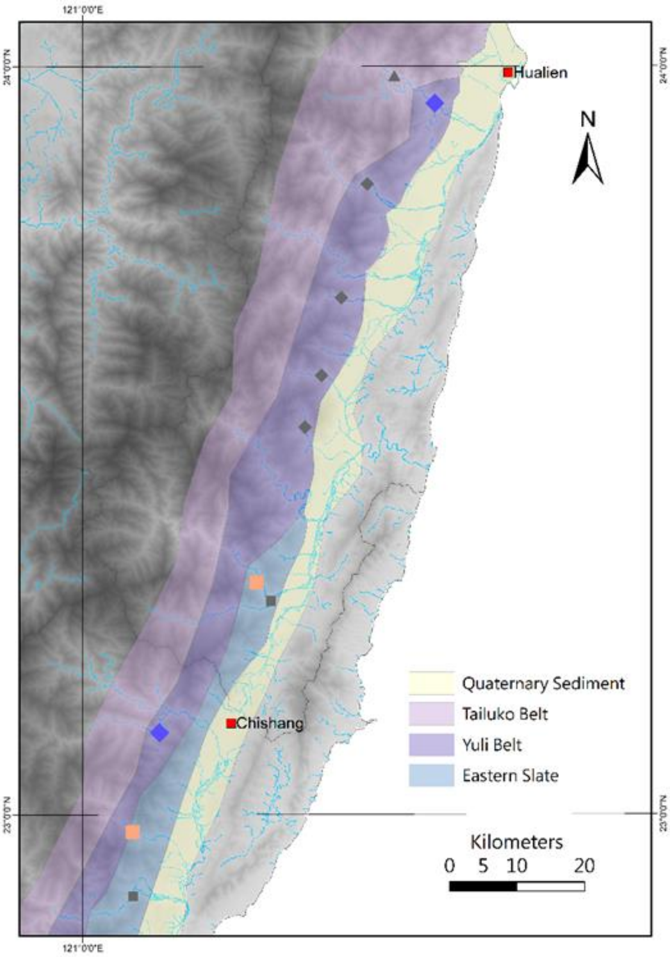

Fig. 2.1 The map of the study area. The gray symbols are from the previous data, colorful ones are from this study data.

2.2 Gentle-dipping Crenulation Cleavage (S3)

2.2.1 Definition:

Taiwan is a typical mountain belt. Along the eastern Backbone Range, S2 with NE-striking and NW-dipping is the most distinctive foliation (Fig.2.1b). During the fieldwork, we further observed a series of foliations that are crenulated S2 and localized with gentle-dipping, we called it S3 hereafter.

2.2.2 Stereograms

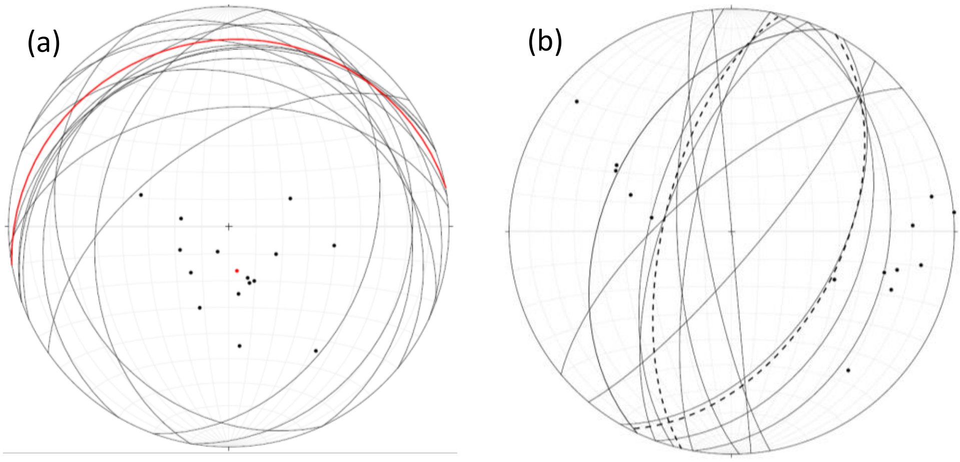

Fig. 2.1 Stereograms. (a) The crenulation cleavages (S3). The red great circle and point is the average attitude 259.9°/16.4°N (n=15), and (b) S2 foliation. Solid and dash great circle are S2 plane and its average plans.

2.2.3 Sample photo

Location	Fieldwork photo	Stereogram
Mukua river		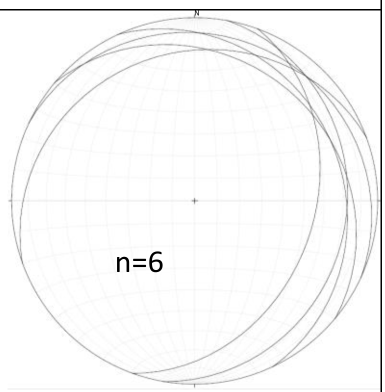
Lele river		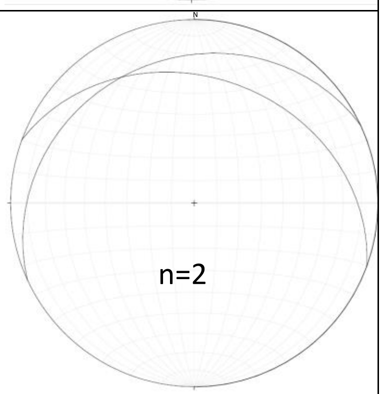

Dalun river		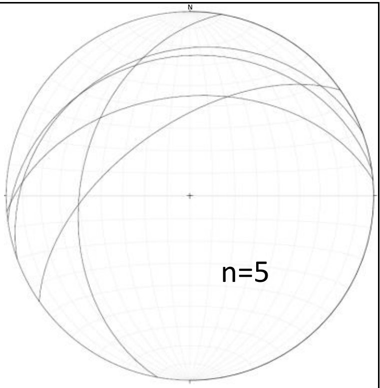
Luliao river		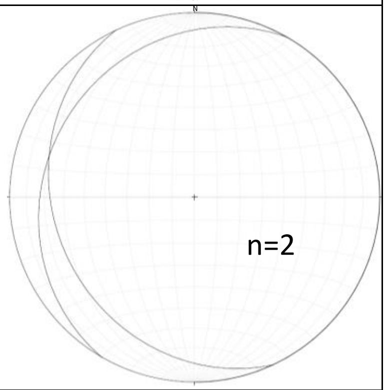

3. Methods and Sampling Strategy

This study focuses on the gentle-dipping crenulation cleavages(S3) that occurred at the eastern Slate Belt, Yuli Belt, and Tailuko Belt in the eastern Backbone Range. We took photographs and collected oriented samples for microstructural observations, shortening calculations, and RSCM analysis.

3.1 Structural Analysis for Shortening

Fieldwork and photographing of S3 were conducted. The images were digitized and the vertical shortening was calculated via the Matlab code (Chen, 2018).

3.1.1 Equation of Shortening

Equation (1) is the definition of elongation. Red line is the distance between two hinge points of axial trace, and yellow line is the original arc length between two hinge points (Fig 3.1).

Shortening = (Red Line – Yellow Line) / Yellow Line. *(1)*

Therefore, by using sin function on shortening for pure shear estimation, and cos function for simple shear. PS is an equation to sub-vertical shortening as the Equation (2).

PS = Shortening × sinϑ *(2)*

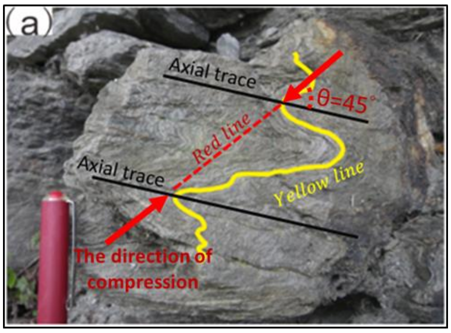

Fig. 3.1 Fold geometry (Chen, 2018)

3.1.2 Data Collection

Field data were recorded during the field work, such as position, the attitude of the axial plane and fold axis, and direction of right-hand side (Fig 3.2).

In order to reduce errors in calculation, the sight direction of the camera should be parallel to the orientation of the fold axis and the bottom of the camera should be horizontal (Fig 3.2; Chen, 2018).

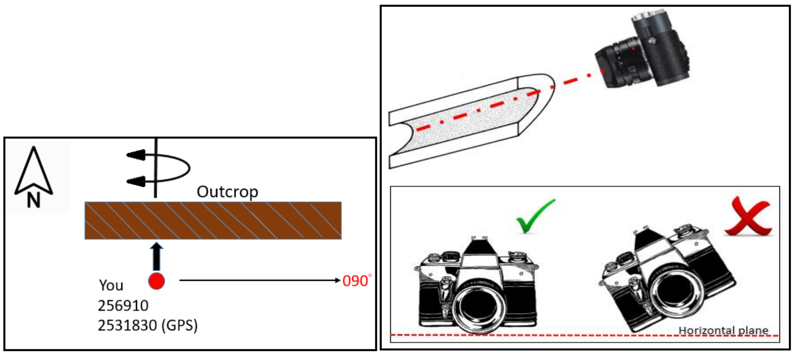

Fig. 3.2 Recording method and the instructions of taking photos (Chen, 2018).

3.1 Raman Spectroscopy on Carbonaceous Materials (RSCM)

The RSCM study was used to evaluate the degree of thermal transformation of carbonaceous materials which is an irreversible process. Thus, the RSCM data can be represented as the maximum temperature during the metamorphic event (Clement et al., 2019; Sun, 2020).

The Raman spectrum of CM is composed of D1, D2, D3, D4, and G bands (Fig. 3.3; Tuinstra & Koenig, 1970; Nemanich & Solin, 1979). With increasing temperature, the D1 and D2 bands decrease relative to the G band, and the D3 band is absent when samples have undergone temperature higher than 400-450°C (Beyssac et al., 2002; Lahfid et al., 2010).

In this study, only the D1, D2, and G were detected within the samples.

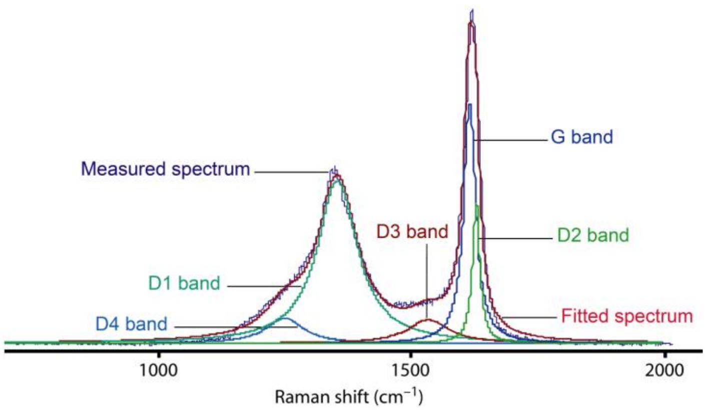

Fig. 3.3 Peak-fitting of the Raman spectrum. This spectrum is composed of the graphite band (G) and four defect bands (D) (Lahfid et al., 2010).

3.2.1 Thin Section

The Raman spectra measured from conventionally petrographic thin sections with a thickness of 30 mm (Beyssac et al., 2002), and roughness less than 30 µm (Sun, 2020). Also, we assumed that the fold axis is the x-axis, therefore, the axial plane of S3 is yz-plane. And, the thin sections should be perpendicular to the foliation and fold axis, which is yz-plane (Fig. 3.4) (Beyssac et al., 2002).

Fig. 3.4 Thin sections of the oriented sample (2020071502) from Mukua river.

3.2.2 Measuring the Raman spectrum of CM

The RSCM study focused on the 800-2000 cm^{-1} region which includes all the CM bands. We repeated the spectrum three times to increase the signal-to-noise ratio and conducted the laser at least 10 times on each target for the confidence of data. Also, we identified the target position of S2 and S3. When CMs formed on or near the black band material, they were identified as S3 targets, and when CMs formed at other space without black material, they were treated as S2 targets. Additionally, to avoid any mechanical disruption of CM, the best solution is to focus the laser on CM situated beneath a transparent grain, for instance quartz or calcite mineral (Beyssac et al., 2003).

3.2.3 RSCM Thermometry

The peak fitting of the spectrum was determined using the computer program Peakfit 4.1.1 after removal of noisy data (Fig 3.5). When obtaining the band areas, the temperature can be estimated through the empirical equation

(Equation 3). The empirical equation of the maximum temperature was selected from Beyssac et al (2002):

$$R2_{\text{Band Area}} = D1/(G+D1+D2) \qquad (3)$$

$$T(°C) = -445*R2+641$$

Number	Target position	Raman spectrum
01 T=456℃	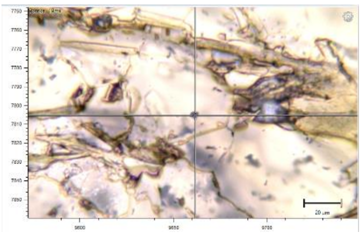	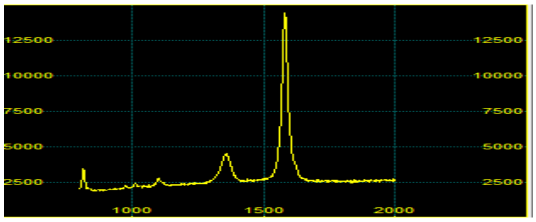
02 T=442℃	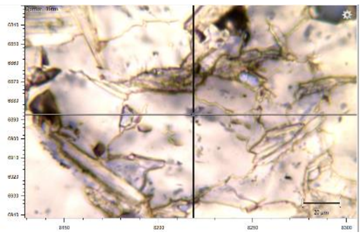	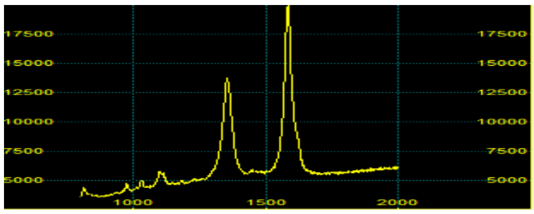
03 T=489℃	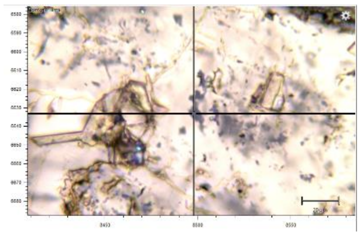	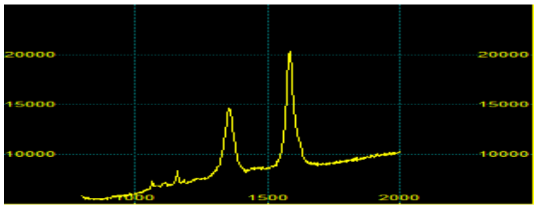
04 T=470℃	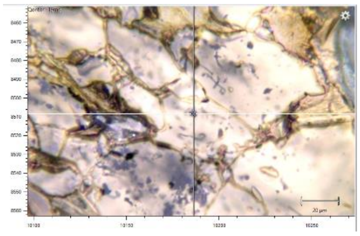	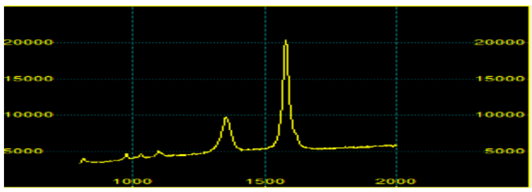

Fig 3.5 Target positions and spectrum of RSCM on the sample 2020071502_S2.

01 T=456℃	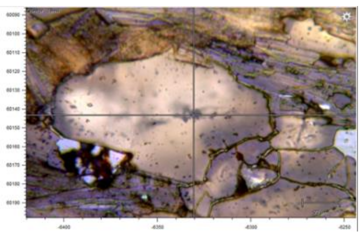	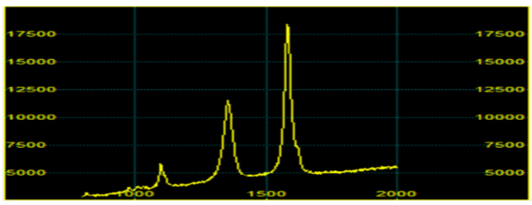

02 T=442℃	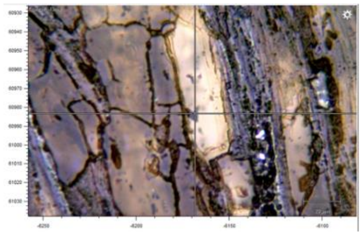	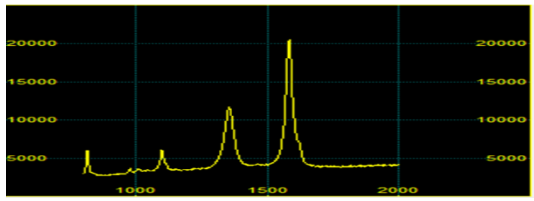
03 T=489℃	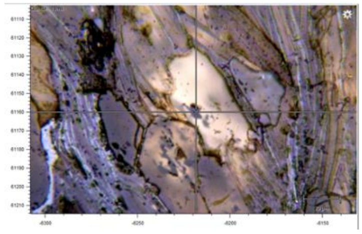	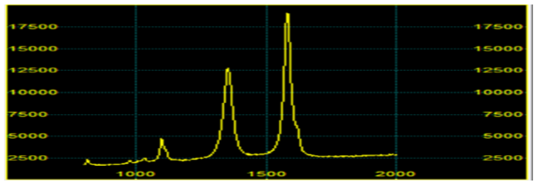
04 T=470℃	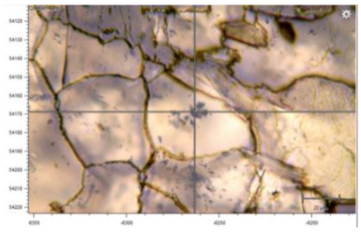	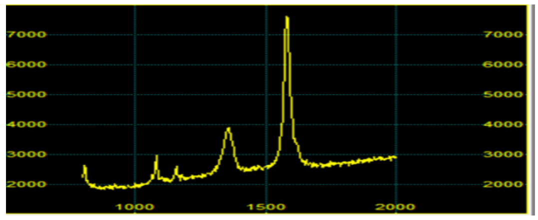
Number	Target position	Raman spectrum

Fig 3.6 Target positions and spectrum of RSCM on the sample 2020071502_S3.

3.2.4 Statistics

Kouketsu et al. (2019) defined two types of the temperature distribution of RSCM, including continuous type and Near-binormal type (Fig 3.7). To realize the impacts of standard deviations, therefore, the statistical analysis of the temperature distribution as the interval of 10°C, 15°C, 20°C was conducted.

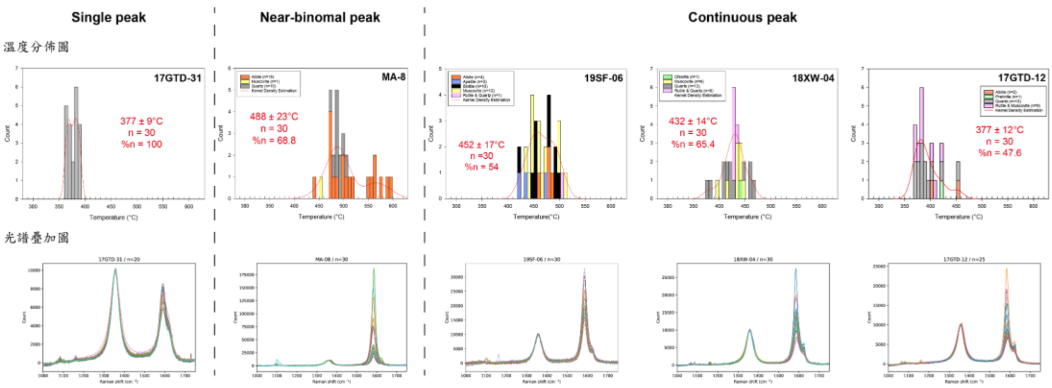

Fig. 3.7 The categories of temperature distribution of RSCM (Lin, 2020).

4. Results

4.1 Subvertical Shortening Analysis

4.1.1 Shortening distribution along the Backbone Range

The average of the subvertical shortening is -0.33, -0.11, -0.20 and -0.55 in the Mukua, Dalun, Lele and Luliao river, respectively (Fig4.1).

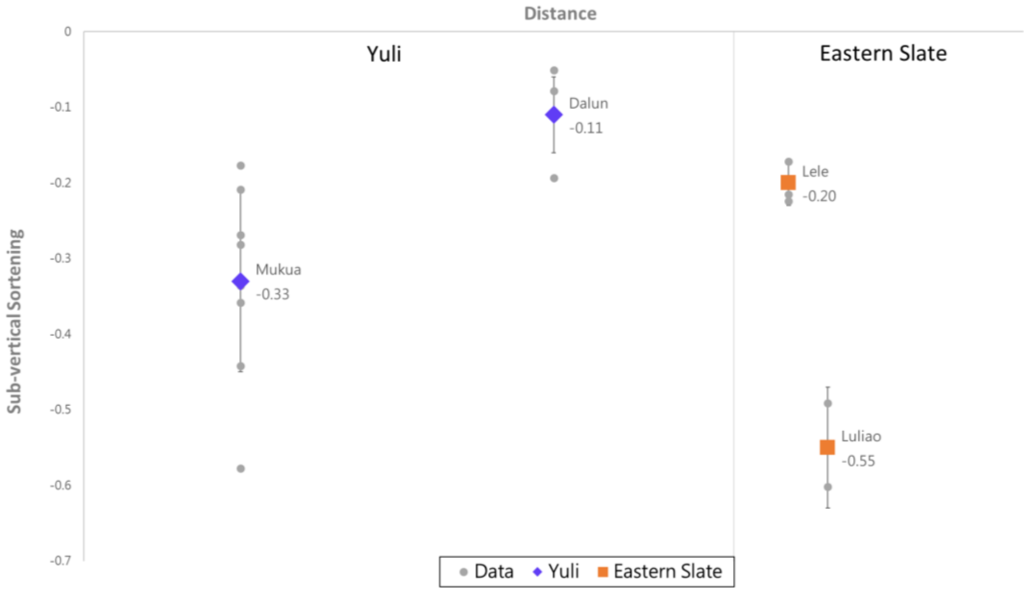

Fig4.1 The subvertical shortening in the different areas.

4.1.2 Shortening distribution among scales

The average of the subvertical shortening is -0.33 in the meso-scale (centimeters) and -0.15 in the micro-scale (micrometer) of the Mukua river (Fig4.2).

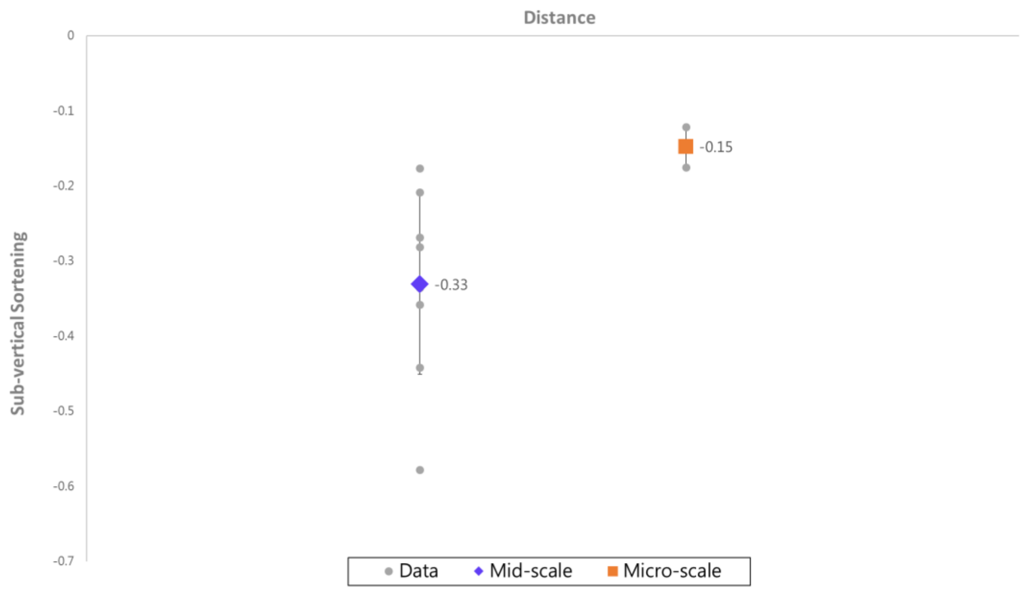

Fig4.2 The subvertical shortening in the micro-scale and mid-scale of the Mukua river.

4.1 Thin Section Observation

Open Nicole	Cross Nicole
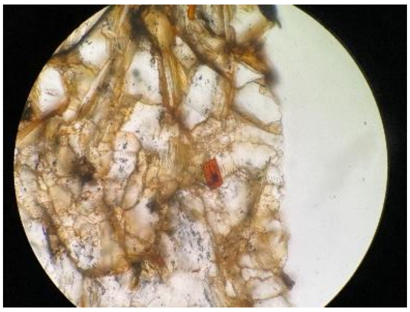	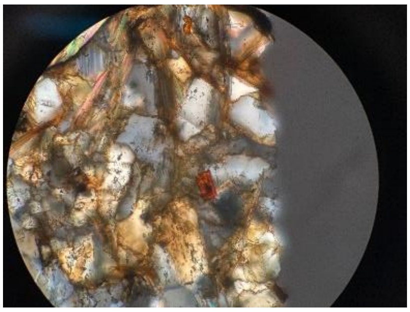
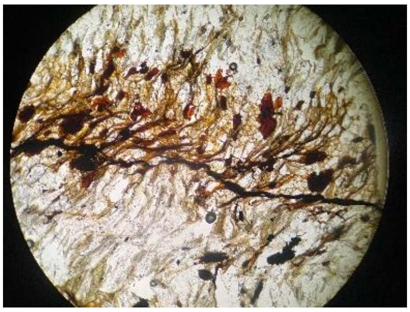	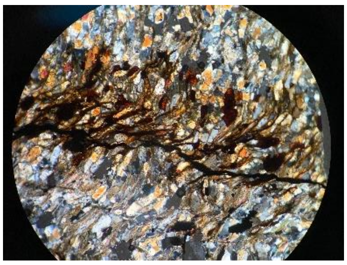

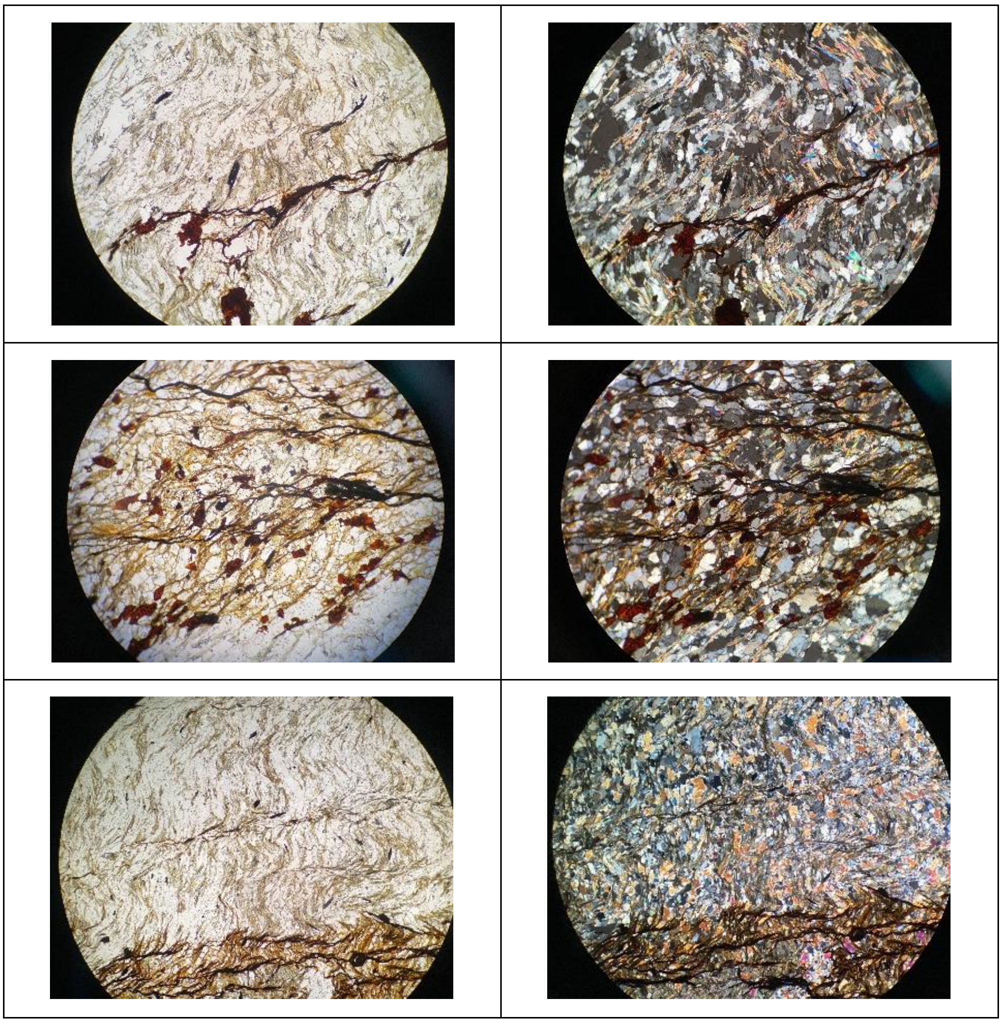

Fig4.3 The thin section observation.

4.3 The maximum metamorphic temperature of RSCM

4.3.1 The maximum metamorphic temperature

The maximum metamorphic temperature of S2 is 463±30°C; S3 is 472±30°C (Table 4.1).

Table4.1 Sample description with RSCM results. * are the strange spectra number, they were deleted in the calculation due to the accuracy and be discussed in section 5.

Sample	Foliation	Lithology	Setting	Position	Number of spectra	Metamorphic temperature	σ	Type of temperature

					(n/*/n+*)	(˚C)		distribution
2020071502	S2	Meta-	Yuli	23°57'4''N	18/4/22	463	±30	Continuous
	S3	sandstone	belt	121°30'45''E	20/13/33	472	±30	Near-binormal

4.3.2 The distribution of temperature

The temperature distribution of S2 shows continuous type (Fig. 4.4); S3 shows near-binormal when the class interval is 15°C and 20°C (Fig.4.5b, c).

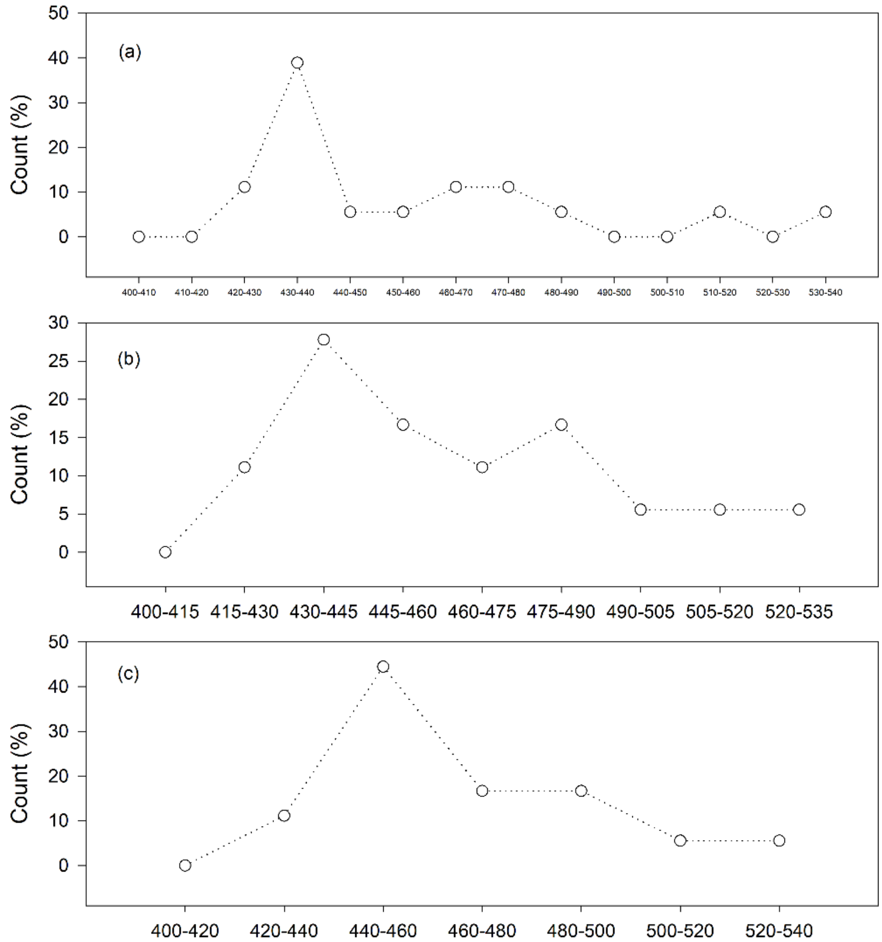

Fig4.4 The temperature distribution of S2 with the class interval by 10˚C (a), 15˚C (b), 20˚C (c).

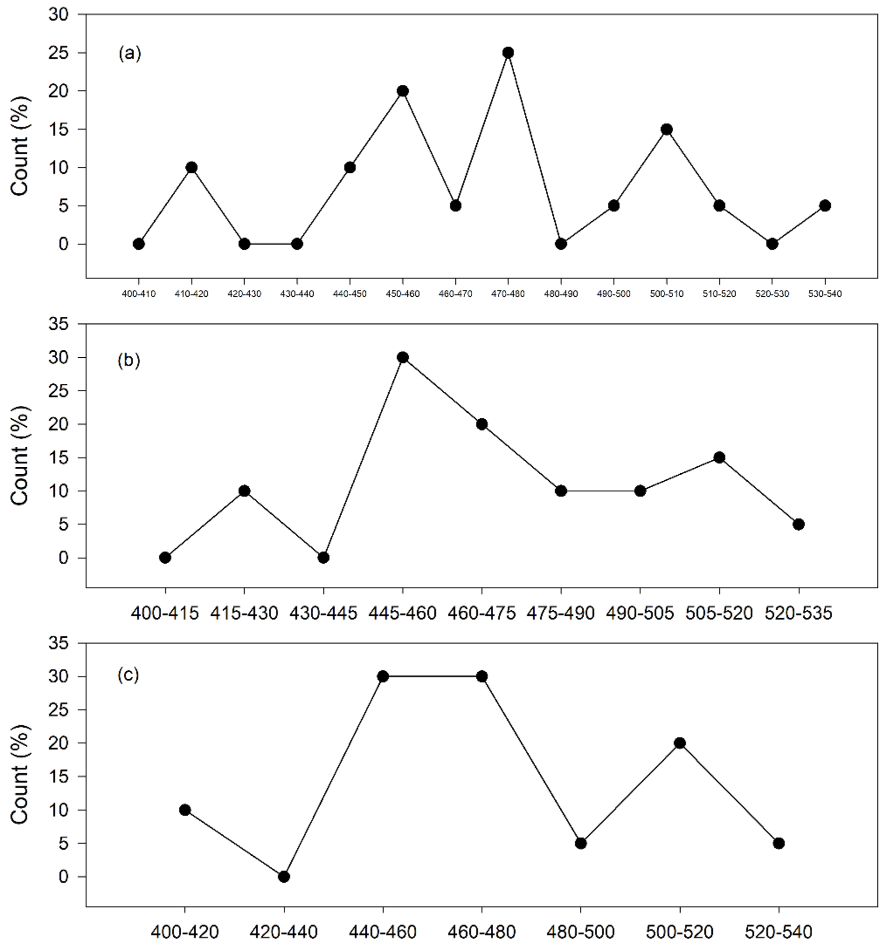

Fig4.5 The temperature distribution of S3 with the class interval by 10°C (a), 15°C (b), 20°C (c).

5. Discussion

5.1 Shortening in different scales and areas

The sub-vertical shortening in three areas are in a similar range (Fig5.1), the largest is at Luliao river which is -0.55.

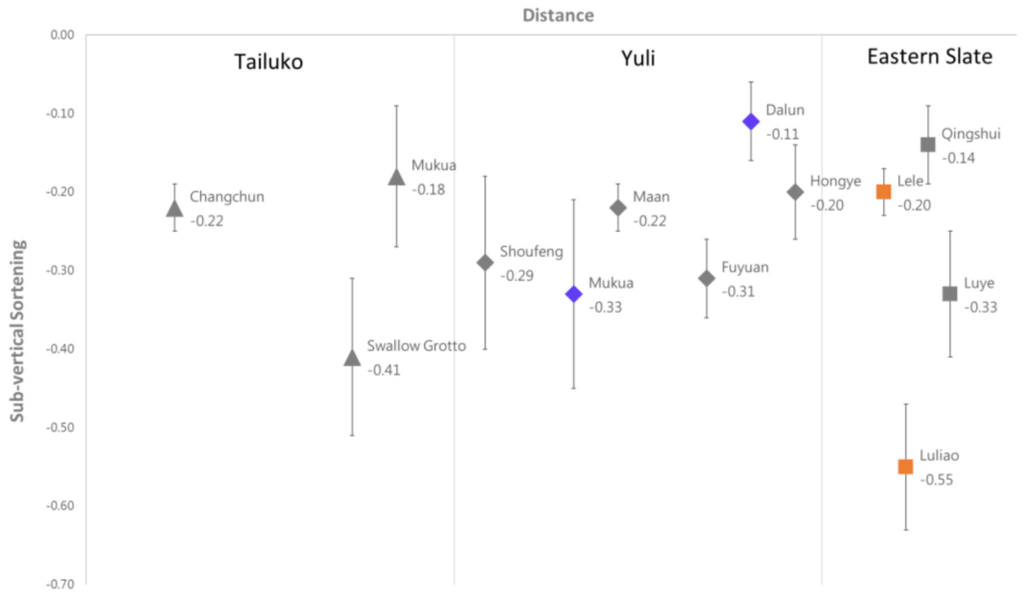

Fig5.1 The sub-vertical shortening diagram. The color spot is from this study data, the gray spot is from Chen (2020).

5.2 The transparent brown minerals in crenulation cleavage(S3)

The transparent brown minerals are analyzed by Raman spectrum, which the possible result is goethite, because we didn't find any texture of goethite under microscope.

5.3 The temperature distribution of RSCM between S2 and S3

The temperature distribution of S3 occurred high temperature peak at 512°C which is relative to the distribution of S2. It showed that something heated was added into S3.

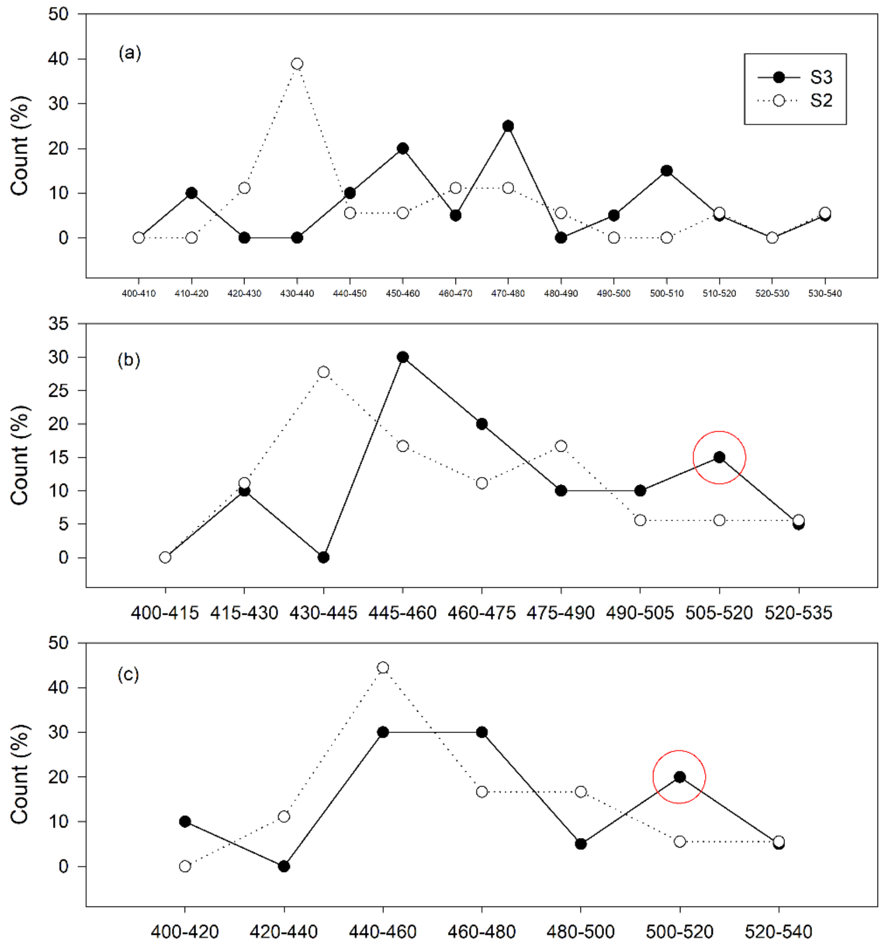

Fig5.2 The temperature distribution of S2 and S3 with the class interval by 10°C (a), 15°C (b), 20°C (c). The red circle marked the peak of relatively high temperature with S3.

6. Conclusion and Future Work

First, the subvertical shortening in the Tailuko belt is -0.25, in the Yuli belt is -0.34 and -0.17, and in the eastern slate belt is -0.59, they are similar among the eastern Backbone Range. Therefore, we can regard the sample at Mukua river as a regional representative. Second, the maximum metamorphic temperatures of S2 is 463±30°C and S3 is 472±30°C at Mukua river. They are higher than the Ar-Ar closure temperature of muscovite (350°C). Therefore, the possibility of obtaining the deformation age of S3 is not so good. Third, the temperature distribution of

RSCM between S2 and S3, which shows a peak at 512.5°C, implied that something heated was added into S3 foliation. Furthermore, the brown minerals in crenulation cleavage(S3) should be identified technically.

References

林翰君（2020），台灣東部玉里帶的變質溫度與構造特性。國立中正大學地球與環境科學系碩士班碩士論文。

孫浩誠（2020），台灣造山帶板岩區的熱變質演化–以紅香到武界為例。國立中央大學地球科學學系碩士論文。

Beyssac, O., Goffé, B., Chopin, C., & Rouzaud, J. N. (2002). Raman spectra of carbonaceous material in metasediments: a new geothermometer. *Journal of Metamorphic Geology, 20*(9), 859-871.

Beyssac, O., Goffé, B., Petitet, J. P., Froigneux, E., Moreau, M., & Rouzaud, J. N. (2003). On the characterization of disordered and heterogeneous carbonaceous materials by Raman spectroscopy. *Spectrochimica Acta Part A: Molecular and Biomolecular Spectroscopy, 59*(10), 2267-2276.

Chen, Y. H. (2018). Study of Exhumation Processes of the Eastern Central Range, Taiwan. Summer project, NTNU, Taiwan.

Conand, C., Mouthereau, F., Ganne, J., Lin, A. T., Lahfid, A., Daudet, M., Mesalles, L., Giletycz, S., & Bonzani, M. (2020). Strain Partitioning and Exhumation in Oblique Taiwan Collision: Role of Rift Architecture and Plate Kinematics. *Tectonics, 39*(4).

Kouketsu, Y., Mizukami, T., Mori, H., Endo, S., Aoya, M., Hara, H., Nakamura, D., & Wallis, S. (2014). A new approach to develop the Raman carbonaceous material geothermometer for low-grade metamorphism using peak width. *Island Arc 23*, 33–50.

Lahfid A., Beyssac O., Deville E., Negro F., Chopinc. & Goffe B. (2010). Evolution of the

Raman spectrum of carbonaceous material in low-grade metasediments of the Glarus Alps (Switzerland). *Terra Nova 22*, 354–60.